Simulation of the chemical potential and the cavity free energy of dense hardsphere fluids

Phil Attard

Citation: J. Chem. Phys. **98**, 2225 (1993); doi: 10.1063/1.464202
View online: http://dx.doi.org/10.1063/1.464202
View Table of Contents: http://jcp.aip.org/resource/1/JCPSA6/v98/i3
Published by the American Institute of Physics.

Simulation of the chemical potential and the cavity free energy of dense hard-sphere fluids

Phil Attard
Department of Applied Mathematics, Research School of Physical Sciences and Engineering, Australian National University, Canberra, Australian Capital Territory, 2601 Australia

(Received 30 July 1992; accepted 5 October 1992)

The chemical potential of dense hard-sphere fluids, and also the work of cavity formation, are simulated directly by a force-balance Monte Carlo technique. Here the coupling between a solute and the solvent varies in the presence of an external field. For a hard-sphere fluid the variable is the cavity diameter, and the scaled particle theory proves sufficient for the applied field. The method is shown to be viable for densities as high as the freezing transition. A vectorizable Monte Carlo computer algorithm is also given.

I. INTRODUCTION

The chemical potential determines the number of molecules per unit volume. It is the most appropriate independent variable for open systems, phase equilibria, for example. Another important use of the chemical potential is in the study of inhomogeneous fluids. For a uniform fluid, one can specify the number of particles in a given volume, and calculate the bulk equation of state. However, when the fluid density varies in space due to the application of an external field, setting the total number of particles does not immediately yield the equilibrium bulk state point, particularly in confined geometries. One needs in addition to calculate the chemical potential (or else to fix it) in order to make a connection between the inhomogeneous fluid and the uniform fluid that it is in equilibrium with.

Molecular simulations provide microscopic detail of model systems, and increasingly ambitious applications are being attempted, including inhomogeneous fluids. The chemical potential can be obtained directly by Monte Carlo methods, specifically by grand canonical Monte Carlo,[1–3] in which particles are created or destroyed, and by Widom's test particle method,[4] where the local field felt by a virtual test particle is found. Both methods become problematic at liquidlike densities because a point chosen completely at random is almost certain to overlap with the cores of the molecules of the dense fluid.

These two original schemes have been modified to improve their utility at higher densities. Mezei[5] gave a cavity-biased approach, where insertions are attempted within cavities in the fluid. Shing and Gubbins[6,7] developed a method involving potential distributions, virtual particles, and restricted umbrella sampling, which is also suitable for molecular dynamics simulations.[8] Mon and Griffiths[9] gradually inserted or deleted a particle by changing the partial interaction of one of the particles with the rest. Cagin and Pettitt gave a grand molecular dynamics method that also involves partial particles.[10]

Recently a particular Monte Carlo technique has been described, where mechanical properties such as the pressure and the surface tension could be obtained from the balance of forces acting on containers or solutes that fluctuate in external fields.[11] One example is to have a solute similar to the solvent molecules, except that it interacts with them via a partial potential with variable coupling. It was shown that the chemical potential could be obtained from such an ensemble, at least in principle.[11] In so far as the method uses a partially coupled solvent molecule it resembles the method of Mon and Griffiths,[9] but it extends that approach in the sense that a continuous range of coupling parameter values are used during one simulation, and that an external field is invoked. The force-balance method for determining the chemical potential was advocated because the partially coupled solvent particle (the solute) is a real particle in the fluid, and hence the probability of accepting a trial move depends in a controlled fashion upon the externally imposed field. This is in contrast to the original methods described above, where the probability of a chance occurrence of a solvent-sized cavity is vanishingly small in dense fluids.

This paper tests the feasibility of the force-balance method for relatively dense hard-sphere fluids. This model system was chosen because it is the simplest nontrivial fluid that displays volume exclusion effects. In addition, it has been extensively studied, both in its own right and as a reference fluid for more realistic systems, and a number of exact and approximate results are known. Adams[2] has previously simulated the chemical potential of hard-sphere fluids for densities up to $\rho d^3=0.8$ using the nearest-neighbor function (an application of Widom's method) and also grand canonical Monte Carlo. In this paper the chemical potential is obtained for densities up to $\rho d^3=0.92$, and comparison is made with several of the approximate theories. In the hard-sphere fluid, the solute particle used in the force balance method is actually a cavity of variable diameter, and in addition to the chemical potential of the bulk hard-sphere fluid, results are obtained for the work of forming the cavity as a function of its diameter. This quantity, which may also be called the free energy of cavity solvation, is also compared which approximate results.

The paper is divided into five sections. Immediately following this introduction is a summary of several approximate theories for the hard-sphere fluid. Section III outlines the force balance technique as applied to the chemical potential. A discussion of a general Monte Carlo algorithm

 0021-9606/93/032225-07$006.00

suitable for vector or parallel computer architectures is included. Section IV contains the exact and approximate results obtained here for the chemical potential and for the cavity free energy. Section V concludes the paper.

II. APPROXIMATE THEORIES

If the equation of state of a fluid is known, then the chemical potential may be evaluated from the expression

$$\mu=\mu_0+\int_{P_0}^{P}\frac{dP'}{\rho'}, \tag{2.1}$$

where P is the pressure and ρ is the density. Several analytic approximations exist for the equation of state of a hard-sphere fluid, including that due to Carnahan and Starling,[12]

$$P_{\rm CS}=\rho k_B T\frac{1+\eta+\eta^2-\eta^3}{(1-\eta)^3}, \tag{2.2}$$

and that given by the scaled particle theory,[13]

$$P_{\rm SPT}=\rho k_B T\frac{1+\eta+\eta^2}{(1-\eta)^3}. \tag{2.3}$$

In these expressions, k_B is Boltzmann's constant, T is the temperature, and $\eta=\pi\rho d^3/6$ is the packing fraction, where d is the hard-sphere diameter. These yield for the excess chemical potential (additional to that of an ideal gas)

$$\beta\mu^{\rm ex}_{\rm CS}=\frac{8\eta-9\eta^2+3\eta^3}{(1-\eta)^3}, \tag{2.4}$$

and

$$\beta\mu^{\rm ex}_{\rm SPT}=-\ln[1-\eta]+\frac{\eta(14-13\eta+5\eta^2)}{2(1-\eta)^3}, \tag{2.5}$$

where $\beta=1/k_BT$.

In the present paper, the scaled particle theory is of special interest because its derivation invokes the work required to form a cavity in the fluid.[13] This is taken to be the pressure times the volume of the cavity, plus the surface free energy of a planar interface times the surface area of the cavity, plus a term proportional to the diameter of the cavity. For a cavity of diameter λd the result is

$$\beta W_{\rm SPT}(\lambda)=\begin{cases}-\ln[1-8\eta\lambda^3] & \lambda\leqslant 1/2,\\ -\ln[1-\eta]+\dfrac{\eta^2(1+\eta+\eta^2)}{(1-\eta)^3}(8\lambda^3-1)- & \\ \dfrac{9\eta^2(1+\eta)}{2(1-\eta)^3}(4\lambda^2-1)+\dfrac{9\eta^3}{(1-\eta)^3}(2\lambda-1) & \lambda>1/2.\end{cases} \tag{2.6}$$

This expression is exact for $\lambda\leqslant 1/2$. Note that the chemical potential of a hard-sphere fluid is just the work of forming a solvent-sized cavity, $\mu^{\rm ex}=W(1)$, and the above scaled particle expressions are consistent in this respect.

There also exist numerical schemes for obtaining the equilibrium properties of fluids. Integral equation approaches are based upon the exact Ornstein–Zernike equation and some approximate closure such as the hypernetted chain. The techniques for solving these equations are well known, including for solutes at infinite dilution in a hard-sphere fluid.[14] Within the hypernetted chain approximation, the solvation free energy may be expressed in terms of the solute–solvent direct (c_{01}) and total (h_{01}) pair correlation functions,[15,16]

$$\beta W_{\rm HNC}(\lambda)=-\rho\int[c_{01}(r;\lambda)-h_{01}(r;\lambda)^2/2+c_{01}(r;\lambda)h_{01}(r;\lambda)]d\mathbf{r}. \tag{2.7}$$

For the case of a cavity in a hard-sphere fluid, the cavity of diameter λd is equivalent to a solute hard sphere of diameter $2\lambda d-d$, although the latter quantity need never actually enter the equations. The excess chemical potential is $\mu^{\rm ex}_{\rm HNC}=W_{\rm HNC}(1)$, and this quantity involves only pure bulk solvent pair correlation functions.

III. FORCE-BALANCE MONTE CARLO

A. Chemical potential

In this section the force-balance method[11] for the determination of the chemical potential is summarized. Consider a fluid of N particles in a volume V at a temperature T. One particle, the solute, is partially coupled to the rest. Its interaction potential is characterized by the parameter λ; at $\lambda=0$ the solute is ideal, and at $\lambda=1$ it is identical to the other solvent particles. The canonical partition function is

$$Q(N,V,T;\lambda)=\frac{\Lambda^{-3N}}{N!}\int_V e^{-\beta H(\mathbf{r}^N;\lambda)}\,d\mathbf{r}_1\cdots d\mathbf{r}_N, \tag{3.1}$$

where Λ is the de Broglie thermal wavelength, $\mathbf{r}_i$ is the coordinate of particle i, and $H(\mathbf{r}^N;\lambda)$ is the configurational part of the Hamiltonian, which is the sum of the interaction potentials of the particles. The Helmholtz free energy is

$$A(N,V,T;\lambda)=-k_BT\ln Q(N,V,T;\lambda), \tag{3.2}$$

and the excess chemical potential is given by (in the thermodynamic limit),

$$\mu^{\rm ex}=A(N,V,T;1)-A(N,V,T;0), \tag{3.3}$$

where the fact that the ideal contributions are unaffected by the coupling parameter has been used.

Now let the coupling fluctuate in the presence of an external potential $\psi(\lambda)$, and define a new ensemble whose partition function is

$$\Theta(N,V,T;\psi)=\int_0^\infty e^{-\beta\psi(\lambda)}Q(N,V,T;\lambda)d\lambda. \tag{3.4}$$

One may define a free energy function,

$$f(\lambda)=A(N,V,T;\lambda)+\psi(\lambda), \tag{3.5}$$

which equals the free energy of the ensemble at the equilibrium coupling, $f(\bar\lambda)=-k_BT\ln\Theta(N,V,T;\psi)$, where it is a minimum, $f'(\bar\lambda)=0$. Here $\bar\lambda$ is the average value of the

coupling in this ensemble, and the prime denotes the derivative. This last result may be written

$$\left.\frac{\partial A(N,V,T;\lambda)}{\partial\lambda}\right|_{\lambda=\bar{\lambda}} = -\psi'(\bar{\lambda}). \tag{3.6}$$

It was pointed out[11] that this allows one to determine the chemical potential of the fluid because Eq. (3.3) may be written

$$\mu^{\rm ex} = \int_0^1 \frac{\partial A(N,V,T;\lambda)}{\partial\lambda}\, d\lambda. \tag{3.7}$$

Hence several simulations with different ψ and hence $\bar{\lambda}$ enable a numerical estimate of $\mu^{\rm ex}$ to be made. This result may be compared with Eq. (2.13) of Ref. 9.

It was also mentioned[11] that one could determine the chemical potential in a single simulation, by using the fact that the probability of a coupling of strength λ occurring for a given external potential is proportional to

$$\mathscr{P}(\lambda) \propto \exp -\beta[A(N,V,T,\lambda)+\psi(\lambda)]. \tag{3.8}$$

Equation (3.5) now yields an expression for the solvation free energy of the partially coupled solute,

$$A(N,V,T;\lambda) - A(N,V,T;0) = -k_BT \ln[\mathscr{P}(\lambda)/\mathscr{P}(0)] - [\psi(\lambda)-\psi(0)]. \tag{3.9}$$

Combining this with Eq. (3.3), one obtains for the excess chemical potential

$$\mu^{\rm ex} = -k_BT \ln[\mathscr{P}(1)/\mathscr{P}(0)] - [\psi(1)-\psi(0)]. \tag{3.10}$$

Provided that $\psi(\lambda)$ is chosen suitably so that the whole range of coupling is sufficiently sampled during the simulation, one can estimate the chemical potential from the relative occupancy of the extremes of the unit interval.

It is straightforward to implement a Monte Carlo procedure for this ensemble using the Metropolis algorithm. One defines a pseudo-Hamiltonian,

$$\mathscr{H} \equiv H(\mathbf{r}^N;\lambda) + \psi(\lambda), \tag{3.11}$$

and a trial move, which can be a particle displacement or a change in coupling, is accepted if the reciprocal of the exponential of its change is greater than a random deviate uniformly distributed on [0,1].

As mentioned in Sec. I, the two methods given here appear to have advantages over the particle insertion method in that one is dealing with continuous functions, and with real test particles actually in the fluid, and that the flexibility of the external potential offers the opportunity to optimize the procedure. In this work the second method proved easy to implement, and only it is examined in detail.

B. External potential

Although the second method above for determining the chemical potential is exact for any external potential *in principle*, acceptable results will only be obtained if the whole range of parameter values are sampled sufficiently during the simulation. In practice this means choosing $\psi(\lambda) \approx -A(N,V,T;\lambda)$, because then $\mathscr{P}(\lambda) \approx$ const, leading to more reliable estimates of $\mathscr{P}(1)$ and $\mathscr{P}(0)$. For the case of the hard-sphere fluid, the coupling constant may be taken to be the diameter of the cavity, and one may choose the scaled particle theory expression for the external potential, $\psi(\lambda) = -W_{\rm SPT}(\lambda)$. It is also convenient to place an upper limit larger than the solvent diameter on the range of values that the cavity diameter can take, which corresponds to an infinite external field for λ beyond this maximum.

More generally, it may be that there is no acceptable approximation available for the solvation free energy of the partially coupled solute. In this case one could envisage a procedure where the external field was continually updated during the simulation, until it converged to the desired quantity. That is, one seeks a uniform distribution of couplings on some interval, and one may attain this by setting the new external potential equal to the negative of the current estimate of the free energy; the latter is obtained via Eq. (3.9) using the current external potential. In some cases it may not be practical to sample the whole of the unit interval in a single simulation, and one may have to use several overlapping stages. These procedures were not required here because the scaled particle theory proved adequate for all the results presented below, even at the highest densities.

C. Vectorizable Monte Carlo algorithm

There are two computer simulation techniques: molecular dynamics, which follows the time evolution of the system via Newton's equations of motion, and Monte Carlo, where ensemble averages are obtained by the principles of statistical mechanics. An increasingly significant advantage of the molecular dynamics approach is that it can run very efficiently on modern vector or parallel computer architectures. This is because the movement of the particles and their mutual forces can be calculated simultaneously for the whole system. On the other hand, the Monte Carlo approach is generally sequential, since the attempt to move a new particle depends upon the fate of the previous one. Below is described a general Monte Carlo algorithm that alleviates this restriction to some extent.

The system volume, $V = L^3$, is subdivided into cubic cells of size l, $l = L/M$. The cells must be larger than the potential cutoff, $l > R_c$, so that only particles in neighboring cells interact. To prevent possible interactions between particles in next-nearest neighbor cells during moves, the size of an attempted particle displacement must be less than halve the difference between l and R_c. This subdivision provides a basis for a spatially based neighbor table, which means that the computer time is linear in the number of particles, rather than quadratic as in crude Monte Carlo.

The particular subdivision into cells at least of size R_c lends itself to vectorization because next-nearest neighboring cells are essentially independent. Trial moves may be attempted simultaneously for one particle in each and every cell that is not mutually adjacent. That is, one consid-

ers moving particles in the cells at the intersection of every second plane perpendicular to the x, y, and z axes, one eighth of the total number of cells. (It is convenient for M to be even.) If the average number of neighboring particles in 27 adjacent cells is n, then one is able to calculate $n(M/2)^3$ interactions simultaneously. For each particle that one is moving, one must count the interactions with the rest of the particles in that cell and in its 26 neighboring cells. Having accepted or rejected the trial moves, one simultaneously considers the next particle in each and every cell of that parity. When all the particles in all these cells are exhausted, one goes on to the cells of the next parity. After eight such cycles, one has attempted to make one move of each of the particles in the system.

Because the vector length is quite large, the calculation of the interactions are very efficient, and the computational burden shifts to the setting up of the vectors of the particles to be moved and their neighbors, which is done in two stages. Initially, the two vectors are subdivided into ranges for each particle to be moved, the length of each range being determined by the number of neighboring particles of the particle to be moved. One vector consists of the indeces of the particles to be moved, the same index being duplicated throughout the relevant range, and the other contains the indeces of the neighboring particles. The formation of the neighbors may be vectorized on either of the two nested loops, that over the 27 neighboring cells, or the loop over the $(M/2)^3$ cells of a given parity. Having accepted or rejected the moves of each particle, one goes on in the second stage to consider the next particle to be moved in each cell. This portion is relatively fast because the list of neighbors is mostly unchanged. Having updated the vector of particles to be moved, in each range of the neighbor vector one replaces the new particle to be moved by the previous one (to avoid self-interactions), and one eliminates the range of any cell where the list of particles to be moved has been exhausted. (Note that the important restriction on the maximum size of a trial move means that any move already accepted during this or previous cycles cannot change the list of possibly interacting neighbors.) This second stage is repeated until one has attempted to move all the particles in all the cells of that parity. One then returns to the initialization stage for cells of a new parity. After one has attempted to move all particles (eight cycles), one updates the cell neighbor table.

The novel feature of the present algorithm is the extension of the well-known neighbor list method to the simultaneous evaluation of cells of the same parity. In tests carried out for a hard-sphere fluid on a Fujitsu vp2200, for 500 particles the parity method was over 85% vectorized, and ran about three times faster than crude Monte Carlo (no neighbor lists). In fact, because of the much shorter vector lengths, the usual neighbor list method without parity ran about a factor of two slower than crude Monte Carlo itself. Because the neighbor list methods scale linearly with the number of particles, whereas crude Monte Carlo is quadratic, the latter rapidly becomes prohibitive for larger systems. Even for 200 hard spheres, the parity method was over 75% vectorized, and took about 3/4 the time of crude Monte Carlo and about 1/5 the time of the conventional neighbor list method. In this case, the vectorizable parts of the parity algorithm ran three times faster in vector mode than in scalar. The superior vector performance of the parity algorithm is expected to increase with the range of the potential.

D. Method

The simulations were performed using the force-balance technique. Periodic boundary conditions, the minimum image convention, and spatially based neighbor tables were used, in conjunction with the vectorizable parity algorithm. The hard-sphere particle moves were accepted if no overlap occurred, and the fluctuations in cavity diameter were accepted according to the Metropolis prescription. The external potential was $\psi(\lambda) = -W_{\mathrm{SPT}}(\lambda)$, Eq. (2.6). In most cases the cavity diameter λ was restricted to the interval [0,1.3], the bin-size used for the averages was 0.1, and the maximum attempted step in cavity diameter was 0.2. In some cases the interval used was [0.4,1.2], since this improves the statistics, and since the cavity free energy is known exactly for smaller diameters. Between 200 and 1024 particles were used in the simulations, and up to 3×10^8 moves were attempted. A cycle consisted of one attempted displacement for each solvent, and one attempted displacement and one attempted size change for the cavity. The standard deviation was estimated from the fluctuations in between 40 and 200 subaverages. The number of cells per edge of the simulation cube, M, was between 4 and 10.

Since it is the solute fluctuations that determine the chemical potential, it is desirable to attempt changes in the coupling more frequently. At the same time, the number of attempted moves of the solute and the neighboring solvent particles should be increased relative to moves of the more distant particles. One such preferential sampling scheme has been described by Owicki and Scheraga.[17] This is based upon a biased random choice of particle to be moved, and is not suited to the parity algorithm described above. Instead a somewhat simpler method was explored, one that is more consistent with the movement of particles in cycles, and with the spatial neighbor table. After each full cycle of one attempt to move all particles and to change the solute coupling, a number of "vicinal" cycles were made, typically 1–5. These each consisted of an attempted move of the solute and all of the solvent particles in the cell containing the solute and in each of the 26 neighboring cells. In order to ensure microscopic reversibility, any attempt to move a particle out of the region occupied by these 27 cells was rejected. After each vicinal cycle, the occupancy table for the 27 cells was updated, and a change in solute coupling was attempted. Limited tests of this preferential sampling scheme showed an improved estimate of the chemical potential for the same total number of configurations.

The numerical solution of the Ornstein–Zernike equations with the hypernetted chain closure was substantially as previously described.[14] The method of fast Fourier transform was used, with 2^{13} grid points and a spacing of $0.01d$. The core discontinuities in the pair correlation func-

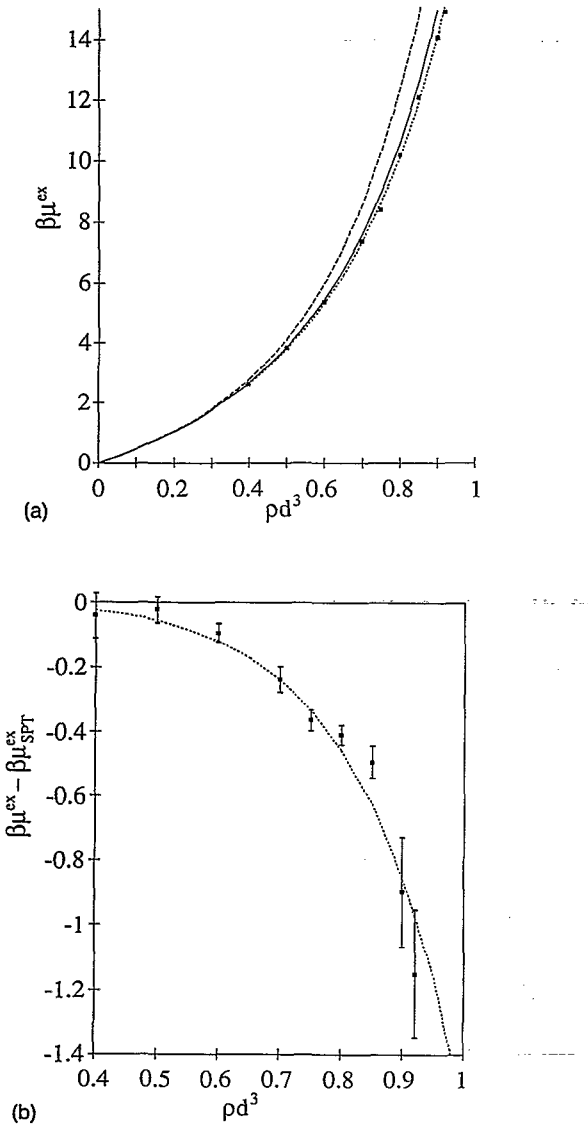

FIG. 1. The excess chemical potential of a hard-sphere fluid as a function of density. (a) The symbols represent the present simulation data, and the curves are the hypernetted chain approximation (dashed), the scaled particle theory (solid), and the Carnahan–Starling equation of state (dotted). (b) Corresponding results less the scaled particle theory prediction.

tions and in their first derivatives were transformed analytically. Six figure convergence was achieved after several hundred iterations at higher densities, where a mixing fraction of about 0.5 was used. The integral for the solvation energy, Eq. (2.7), was evaluated using Simpson's rule.

IV. RESULTS

Figure 1(a) compares the excess chemical potential with that predicted from the various approximations. In general, the chemical potential is a rapidly increasing function of density, and all of the approximations begin to fail at high densities. The hypernetted chain results, which agree with earlier calculations,[18] overestimate the excess chemical potential by about 20% at $\rho d^3=0.8$. The bulk pressure is relatively too large in this approximation by

TABLE I. Monte Carlo results for the excess chemical potential of a hard-sphere fluid at various densities, and for the derivative of the cavity free energy. N is the number of atoms, M is the millions of configurations generated, and the estimated standard deviation of the last digit is in parentheses.

ρd^3	N	M	$\beta\mu^{ex}$	$\bar{\lambda}$	$\beta W'(\bar{\lambda})$
0.4	200	200	2.63(7)	0.66	3.3
0.5	200	79	3.84(4)	0.66	4.8
0.6	200	30	5.34(6)	0.69	7.5
0.6	500	300	5.35(3)	0.81	11.8
0.7	200	69	7.49(8)	0.73	12.1
0.7[a]	500	143	7.36(4)	0.83	17.7
0.75[a]	500	300	8.61(3)	0.85	22.9
0.8	200	50	10.4(1)	0.72	16.2
0.8	500	160	10.38(5)	0.86	27.7
0.8[a]	500	152	10.20(3)	0.87	29.0
0.85[a]	500	225	12.08(5)	0.88	36.2
0.9	20	60	13.8(2)	0.90	46.8
0.9	500	50	13.5(3)	0.93	50.5
0.9[a]	500	45	14.1(2)	0.91	47.5
0.9	1024	250	13.6(2)	0.83	35.8
0.92[a]	500	200	14.9(2)	0.98	64.0

[a]Preferential sampling, four vicinal cycles.

about the same amount, and this approach is more suited for fluids with soft, finite-ranged potentials than for hard-sphere fluids. The scaled particle theory[13] also overestimates the chemical potential, by about 5% at $\rho d^3=0.8$. In this case the approximate bulk pressure is too large by about 10%, and there appears to be some cancellation of errors in this approximation. Since the scaled particle theory is known to provide a relatively accurate description of the surface tension of a hard-sphere fluid at a hard wall,[11,19] the source of these additional errors is probably either in the value of the Tolman length, or in the neglected higher order terms in the expansion (2.6).

Figure 1(b) shows the departure of the excess chemical potential from the scaled particle theory, as given by the simulations and the Carnahan–Starling equation of state.[12] On this expanded scale it can be seen that there is good agreement with the Carnahan–Starling equation of state. Adams[2] found that at high densities Carnahan–Starling underestimated the chemical potential, which is consistent with the very accurate simulations of Erpenbeck and Wood,[20] who found that it underestimated the hard-sphere equation of state.

The simulation results are collected in Table I. Various numbers of particles were employed in an effort to check for the effects of finite size, but these appear to be less than the statistical error. The standard deviation may be slightly underestimated in the case of uniform sampling; there is evidence of correlation between the subaverages. In the case of preferential sampling, the error estimate appears more reliable. The data at $\rho d^3=0.8$ and 0.9 indicate that preferential sampling reduces the statistical error by at least a factor of 2 for the same total number of configurations. The chemical potential was estimated from the free energy of cavity formation using linear and quadratic interpolation. The difference between these, which is the er-

ror due to the finite width of the bins, appeared comparable to the statistical error.

Torrie and Patey[21] simulated the interaction between two cavities in a hard-sphere fluid, and estimated the excess chemical potential from the pair cavity function at zero separation. At the density of $\rho d^3=0.8$, they obtained $\beta\mu^{ex}=9.9$ for 108 particles, and $\beta\mu^{ex}=10.13$ for 864 particles, in reasonable agreement with the results in Table I (10.4 ± 0.1 and 10.20 ± 0.03, for 200 and 500 particles, respectively). Adams[2] found $\beta\mu^{ex}=10.39$ and 10.21 for 32 and 256 particles, respectively. The Carnahan–Starling prediction is 10.15, and that due to the Erpenbeck–Wood equation of state is 10.18.

Also included in Table I is the average diameter of the cavity, and the derivative of the solvation energy at this diameter, Eq. (3.6). Since the diameter of the cavity was restricted to the range [0,1.3], (for the case of 200 particles), a uniform sampling of the interval would lead to $\bar{\lambda}=0.65$. At higher densities the average cavity size is rather larger than this, which indicates that more configurations with the cavity at the upper end of the interval occurred in the simulation. This is because the scaled particle expression, whose negative was used as the external potential, overestimates the work of cavity formation at higher densities and diameters.

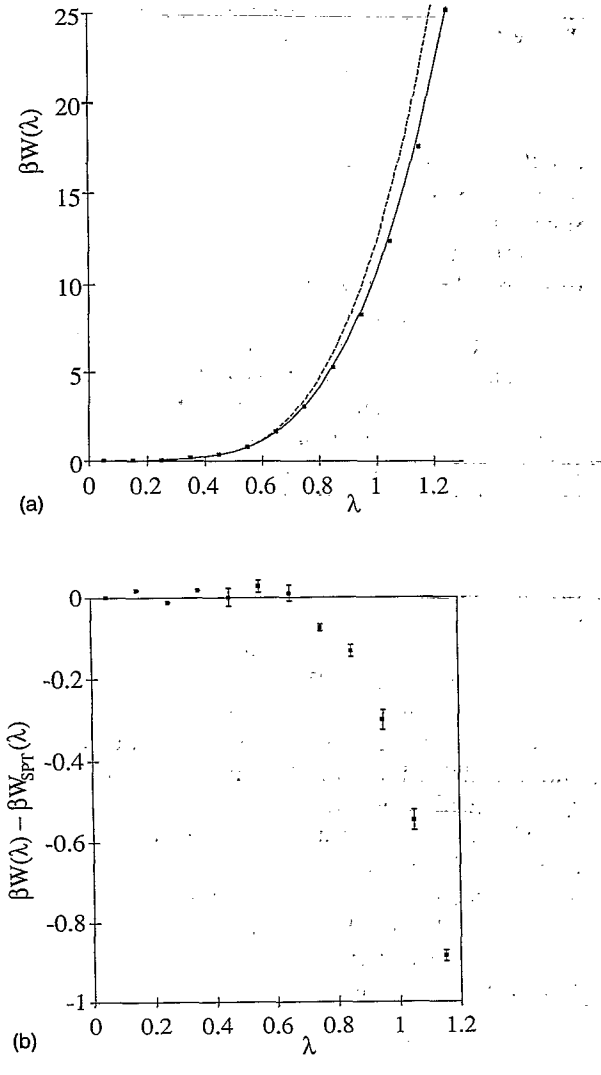

FIG. 2. The work of cavity formation in a hard-sphere fluid ($\rho d^3=0.8$) as a function of cavity diameter. (a) The symbols represent the present simulation data, the dashed curve is the hypernetted chain approximation, and the solid curve is the scaled particle theory. (b) The simulation data less the scaled particle theory prediction.

TABLE II. Monte Carlo results for the cavity free energy, $\beta W(\lambda)$, in hard-sphere fluids at various densities, ρd^3.

	ρd^3								
λ	0.4	0.5	0.6	0.7	0.75	0.8	0.85	0.9	0.92
0.55	0.4	0.4	0.5	0.7	0.7	0.8	0.9	0.9	1.0
0.65	0.7	0.8	1.0	1.3	1.5	1.6	1.9	2.0	2.2
0.75	1.0	1.3	1.8	2.4	2.7	3.0	3.6	3.8	4.3
0.85	1.6	2.1	2.9	3.9	4.5	5.1	6.1	6.8	7.5
0.95	2.2	3.2	4.4	6.0	7.0	8.1	9.8	11.0	12.1
1.05	3.1	4.6	6.4	8.9	10.4	12.2	14.7	16.8	18.3
1.15	4.3	6.3	8.9	12.6	14.8	17.5	21.1	24.7	26.4
1.25	5.7	8.4	11.9	16.9		23.2	28.2	35.9	

The work of cavity formation is plotted in Fig. 2(a) at a density of $\rho d^3=0.8$. The increase with cavity diameter is extremely rapid. Indeed, the scaled particle theory shows that it goes like the pressure times the third power of the diameter. It may be seen from the figure that the hypernetted chain approximation significantly overestimates the solvation free energy, but that on the scale of the figure the scaled particle theory is indistinguishable from the simulation results.

Figure 2(b) shows the difference between the simulation results for the work of cavity formation and the scaled particle theory. For $\lambda\leqslant0.5$ the latter is exact. As the cavity diameter increases, the scaled particle theory systematically overestimates the free energy, in agreement with the findings of Adams.[2] This observation is consistent with the above discussion of its overestimate of the chemical potential, due mainly to using too large a value for the bulk pressure. It is interesting to note that even though the error in the scaled particle theory for the cavity work is less than about one percent (a few tenths of k_BT), when used for the external potential this is enough to cause the solute to be at the upper end of its size range during most of the simulation (see the discussion of $\bar{\lambda}$ following Table I). The simulation data for the solvation free energy of cavities of various diameters over the range of fluid densities are given in Table II.

V. CONCLUSION

This paper has been concerned with the direct simulation of the chemical potential of a hard-sphere fluid, and with the work of cavity formation. Results were obtained for densities up to $\rho d^3=0.92$, and for cavity diameters up to $1.25d$. It was found that the hypernetted chain approximation overestimated the chemical potential and the cavity work, and that the scaled particle theory[13] was better but also too large. The simulation results were in good agreement with the Carnahan–Starling[12] equation of state.

The dense hard-sphere fluid represents a good test of the force-balance Monte Carlo technique for the chemical potential.[11] The latter is calculated directly in a single simulation, in contrast to indirect methods, which involve temperature or density integration [e.g., Eq. (2.1)]. The present results indicate that the method is feasible at quite high densities, and they extend the earlier simulations of Adams, who used both grand canonical Monte Carlo and Widom's test particle method.[2] Although the system sizes and the number of configurations generated are larger here, the statistical error for the chemical potential appears worse because only one in every N configurations involved an attempted cavity size change. Consequently, a preferential sampling scheme (a simplified version of that due to Owicki and Scheraga[17]), suited to the present vectorizable algorithm, was tested, and improved statistics were obtained. With preferential sampling, the force-balance method becomes more tractable. Compared to previous methods, there appears little reduction in the statistical error, and so the main advantage of the force-balance technique is probably its ability to treat dense fluids.

The force balance technique for the chemical potential[11] most closely resembles the method of Mon and Griffiths,[9] who split the insertion of a particle into small discrete changes in the solute–solvent coupling, and so obtained the chemical potential from a series of simulations, one for each step. Hence the present approach may be viewed as the continuous analog of that method, applied in a single simulation. The advantage of allowing small changes in coupling, compared to the insertion of a whole particle, is particularly marked for the hard-sphere fluid, which interacts with a discontinuous potential. This also suggests that the method will work well for fluids that interact with continuous potentials, provided that an efficient external potential is available.

The external field, which is used to balance the fluctuations in the solute coupling, may be considered as an umbrella sampling technique,[21,22] albeit with a particular physical interpretation for certain cases. It may be optimized to extend and to make more uniform the range of the fluctuations in the chemical potential simulations, or in other cases to minimize the variance in thermodynamic averages.[11] In the present case of a cavity in a hard-sphere fluid, the scaled particle theory provided a suitable analytic approximation. More generally, one may have to experiment, or to use a self-consistent numerical scheme as discussed in the text. In any case, the present investigation indicates that the force-balance technique is a viable method of determining the chemical potential of dense fluids.

ACKNOWLEDGMENT

The data reported here were obtained using the Fujitsu VP of the ANU Supercomputer Facility.

[1] G. E. Norman and V. S. Filinov, High Temp. (USSR) **7**, 216 (1969).
[2] D. J. Adams, Mol. Phys. **28**, 1241 (1974).
[3] G. M. Torrie and J. P. Valleau, J. Chem. Phys. **73**, 5807 (1980).
[4] B. Widom, J. Chem. Phys. **39**, 2808 (1963).
[5] M. Mezei, Mol. Phys. **40**, 901 (1980).
[6] K. S. Shing and K. E. Gubbins, Mol. Phys. **43**, 717 (1981).
[7] K. S. Shing and K. E. Gubbins, Mol. Phys. **46**, 1109 (1982).
[8] J. G. Powles, W. A. B. Evans, and N. Quirke, Mol. Phys. **46**, 1347 (1982).
[9] K. K. Mon and R. B. Griffiths, Phys. Rev. A **31**, 956 (1985).
[10] T. Cagin and B. M. Pettitt, Mol. Simul. **6**, 5 (1991).
[11] P. Attard and G. A. Moule, Mol. Phys. (in press).
[12] N. F. Carnahan and K. E. Starling, J. Chem. Phys. **51**, 635 (1969).
[13] H. Reiss, H. L. Frisch, and J. L. Lebowitz, J. Chem. Phys. **31**, 369 (1959).
[14] P. Attard and G. N. Patey, J. Chem. Phys. **92**, 4970 (1990).
[15] T. Morita, Prog. Theor. Phys. **23**, 829 (1960).
[16] P. Attard, J. Chem. Phys. **94**, 2370 (1991).
[17] J. C. Owicki and H. A. Scheraga, Chem. Phys. Lett. **47**, 600 (1977).
[18] R. Kjellander and S. Sarman, J. Chem. Phys. **90**, 2768 (1989).
[19] J. R. Henderson and F. van Swol, Mol. Phys. **51**, 991 (1984).
[20] J. J. Erpenbeck and W. W. Wood, J. Stat. Phys. **35**, 321 (1984); **40**, 787 (1985).
[21] G. Torrie and G. N. Patey, Mol. Phys. **34**, 1623 (1977).
[22] G. M. Torrie and J. P. Valleau, Chem. Phys. Lett. **28**, 578 (1974).